# TECHNICAL
# REPORT

colour
inside

**Fibre optic interconnecting devices and passive components –
Part 03-01: Reliability – Design of an acceptance test for fibre pistoning failure
of connectors during temperature and humidity cycling: demarcation analysis**

## About IEC publications

The technical content of IEC publications is kept under constant review by the IEC. Please make sure that you have the latest edition, a corrigenda or an amendment might have been published.

- Catalogue of IEC publications: www.iec.ch/searchpub

The IEC on-line Catalogue enables you to search by a variety of criteria (reference number, text, technical committee,…). It also gives information on projects, withdrawn and replaced publications.

- IEC Just Published: www.iec.ch/online_news/justpub

Stay up to date on all new IEC publications. Just Published details twice a month all new publications released. Available on-line and also by email.

- Electropedia: www.electropedia.org

The world's leading online dictionary of electronic and electrical terms containing more than 20 000 terms and definitions in English and French, with equivalent terms in additional languages. Also known as the International Electrotechnical Vocabulary online.

- Customer Service Centre: www.iec.ch/webstore/custserv

If you wish to give us your feedback on this publication or need further assistance, please visit the Customer Service Centre FAQ or contact us:

Email: csc@iec.ch
Tel.: +41 22 919 02 11
Fax: +41 22 919 03 00

![IEC logo]

# IEC/TR 62627-03-01

Edition 1.0   2011-04

# TECHNICAL
# REPORT

colour
inside

**Fibre optic interconnecting devices and passive components –
Part 03-01: Reliability – Design of an acceptance test for fibre pistoning failure
of connectors during temperature and humidity cycling: demarcation analysis**

# CONTENTS

INTERNATIONAL ELECTROTECHNICAL COMMISSION
_____

**FIBRE OPTIC INTERCONNECTING
DEVICES AND PASSIVE COMPONENTS –**

**Part 03-01: Reliability – Design of an acceptance test for fibre pistoning
failure of connectors during temperature and humidity cycling:
demarcation analysis**

## FOREWORD

The main task of IEC technical committees is to prepare International Standards. However, a technical committee may propose the publication of a technical report when it has collected data of a different kind from that which is normally published as an International Standard, for example "state of the art".

IEC 62627-03-01, which is a technical report, has been prepared by subcommittee 86B: Fibre optic interconnecting devices and passive components, of IEC technical committee 86: Fibre optics.

The text of this technical report is based on the following documents:

| Enquiry draft | Report on voting |
|---|---|
| 86B/2996/DTR | 86B/3038/RVC |

Full information on the voting for the approval of this technical report can be found in the report on voting indicated in the above table.

This publication has been drafted in accordance with the ISO/IEC Directives, Part 2.

A list of all parts of the IEC 62627 series, published under the general title *Fibre optic interconnecting devices and passive components,* can be found on the IEC website.

The committee has decided that the contents of this publication will remain unchanged until the stability date indicated on the IEC web site under "http://webstore.iec.ch" in the data related to the specific publication. At this date, the publication will be

• reconfirmed,
• withdrawn,
• replaced by a revised edition, or
• amended.

A bilingual version of this publication may be issued at a later date.

**IMPORTANT – The 'colour inside' logo on the cover page of this publication indicates that it contains colours which are considered to be useful for the correct understanding of its contents. Users should therefore print this document using a colour printer.**

# INTRODUCTION

Fibre optic connectors rely on accurate positioning of the fibre with respect to an optical interface to achieve and maintain acceptable performance. Degradation of performance due to fibre motion (fibre pistoning) is a well known failure mode. It is activated by temperature and humidity exposure, especially cyclic. Clause 3 provides background on the pistoning failure mode.

An acceptance test is an accelerated test designed to detect degradation or failure modes if they would occur during life, and to show no change if no degradation or failure modes will occur. A perfect acceptance test is impossible [1][1] because (a) there can always be non-accelerable failure modes and (b) some failures may occur under acceleration that may not occur in service. However, a well-designed acceptance test provides for a supplier a reasonable check of the space of accelerable modes and is of great value in testing for reliability.

Demarcation mapping provides a method of viewing possible chemical and physical processes that can occur during a given stress exposure over a given time [1-4] and allows for selection of accelerating test conditions that will produce potential degradation or failure mechanisms during service. Clause 2 provides an overview of the demarcation approach and its application to developing acceptance tests.

Clause 3 provides a discussion of plausible physical processes accompanying degradation and fibre pistoning, based on an assumed service environment. It includes some models based on these processes, and mathematical tools necessary to develop the demarcation maps. Clause 4 summarizes the results of a numerical experiment, using demarcation maps for each of the processes developed in Clause 3, to compare 20-year life in an extreme tropical climate with accelerated tests.

---

[1]  Figures in square brackets refer to the Bibliography.

# FIBRE OPTIC INTERCONNECTING
# DEVICES AND PASSIVE COMPONENTS –

## Part 03-01: Reliability – Design of an acceptance test for fibre pistoning failure of connectors during temperature and humidity cycling: demarcation analysis

## 1   Scope

This part of IEC 62627 gives an example of the design of an acceptance test for ferrule style connectors when the dominant failure mode is fibre pistoning. The example applies to connectors which use epoxies or other adhesive polymers to bond the fibre into a ferrule. It combines existing evidence, mechanistic hypotheses and the demarcation approximation to develop an accelerated environmental exposure sequence that can be used on a pass-only basis to help ensure reliable service. This technical report was developed to serve only as an example of how accelerated acceptance tests can be designed. It is not intended as a normative standard for any specific application.

## 2   Optical fibre connectors and the pistoning failure mode

The most commonly used fibre optic connector designs are based on butt-joint fibre alignment. The fibre is generally adhesively-bonded inside a tightly toleranced ferrule capillary with a thermally cured epoxy. The ferrule is precision polished to ensure accurate positioning of the fibre endface for acceptable optical performance. Significant fibre motion during temperature-humidity exposure, especially cycling, will degrade the performance, causing both insertion loss and reflectance to increase and become unstable.

The stresses that drive fibre motion come from three sources: (i) residual stress from the connector termination process, (ii) externally applied contact stress from a mating ferrule, or (iii) and stress from differential thermal expansion of materials in the connector assembly. Mechanisms within the adhesive which allow the motion to take place include creep, adhesive failure and cohesive failure.

## 3   Demarcation map theory for thermally activated processes

### 3.1   Concept of demarcation energy

The demarcation approximation is derived from consideration of material systems where a macroscopically observable degradation process is driven by a set of parallel thermally activated (Arrhenius) processes. Assuming each process to consist of a single step, the rate for each local process has the form:

$$k_1 = v\exp\left(\frac{-E_a}{kT}\right)$$

(1)

where

$v$      is a premultiplier,

$k$      is Boltzmann's constant,

$T$      is absolute temperature, and

$E_a$     is the activation energy (in the following, all activation energies are given in eV).

The relative amount (normalized to total amount which can react, also called the reaction *extent*) reacted over time for this local process then has the form:

$$\left(1 - \exp\left(-k_1 t\right)\right) \tag{2}$$

The value of Equation (2), for a given time, temperature and $v$, is plotted across activation energies in Figure 1 and compared to the approximation:

$$\Delta(k_1, t) = \begin{cases} 0, k_1 t < 1 \\ 1, k_1 t \geq 1 \end{cases} \tag{3}$$

The centre vertical line in Figure 1 is the approximation and the circles are the exponential function calculated at discrete activation energies. The two outer vertical lines corresponds to values of $v$ separated by two orders of magnitude, bounds which are important in the following discussions.

The comparison of Equations (2) and (3) shows that $k_1 t = 1$ is a reasonable demarcation between reactions which are complete and those which are not. Substitution from Equation (1) gives the demarcation approximation of Equation (4).

$$E_a = kT \ln(vt) \tag{4}$$

For fixed values of time and temperature, Equation (4) gives the relationship between $E_a$ and $v$, where $E_a$ is the activation energy below which reaction processes are complete and above which they are not. This provides a tool for comparing reactions at potential test times and (accelerating) temperatures with those of actual service conditions. Note that the approximation in this figure does not depend on there being a distribution of activation energies.



IEC  691/11
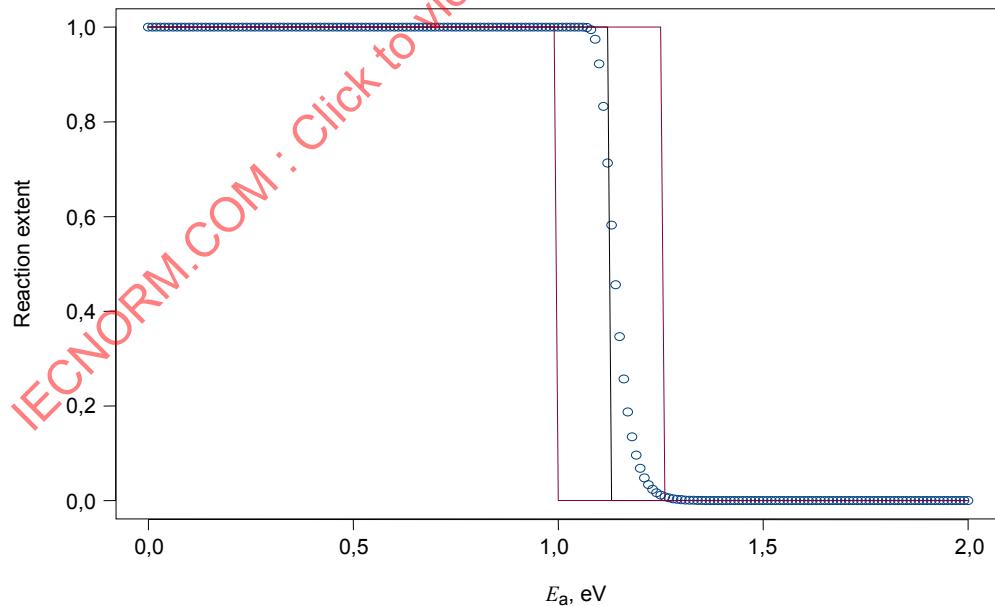
**Figure 1 – Reaction extent as a function of activation energy compared to the $\Delta k_1 t$ function**

## 3.2    Demarcation maps

With the demarcation approximation of Equation (4), it is possible to map the boundaries of completed reactions under given conditions of time and temperature in the two-dimensional space of $E_a$ and $\ln v$ and compare service life and accelerated tests conditions. For the simple case of time at a fixed temperature, the boundaries are straight lines. For the more general case where service or test temperatures are not constant, the demarcation boundaries take a different form. For each value of $v$ time at one temperature can be transformed to an equivalent time at a different temperature corresponding to the same value of $E_a$ as follows:

$$kT_1 \ln(vt_1) = E_a = kT_2 \ln(vt_2) \tag{5}$$

or

$$t_1 = \frac{(vt_2)^{T_2/T_1}}{v} \tag{6}$$

which implies that after a step in temperature, Equation (4) can be re-expressed:

$$E_a = kT_2 \ln\left(v\left(t_2 + \frac{(vt_1)^{T_1/T_2}}{v}\right)\right) \tag{7}$$

A transformation such as Equation (7) can be applied to situations such as the example of a product which is first baked at 180 °C for 4 h, followed by 25 years service at 50 °C. Such a product might be a device requiring metallization [11] of the fibre, or a fibre Bragg grating [3], either of which might require a stabilization anneal. The demarcation map for this product is shown in Figure 2. Clearly these temperatures are not appropriate for epoxy based connectors, however the visual illustration is clearer for these more extreme temperatures. The area above and left of line 1 corresponds to those reactions completed by the bake and those within the shaded area correspond to those reactions subsequently completed by the 25 years service. This can be compared to an accelerated test consisting of the same bake followed by 5 h exposure at 260 °C. The region between curves 1 and 2 corresponds to those reactions completed during the 260 exposure °C after the bake. This accelerated test region includes all reactions occurring during life for values of $v$ greater than $10^3$.



IEC   692/11
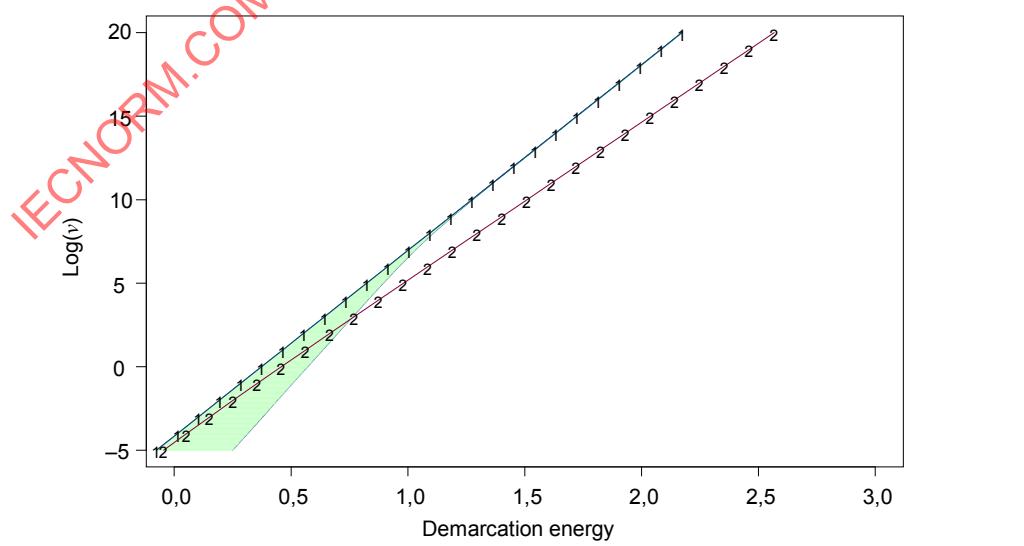
**Figure 2 – Demarcation maps for service life and accelerated test of example in 4.2**

If the goal is to design an acceptance test, it is important for the test to provide coverage for all the processes which might occur during life, while minimizing the chances of rejecting a good material system, with the minimum cost and time expenditure. The plot and discussion above suggest a single number that can be extracted from the demarcation maps which provides a simple characterization of the degree of conservativeness of the accelerated test with respect to accelerable failure modes. That number is the minimum value of $\nu$ where the accelerated test contains all the processes occurring during life. This is the simplest use of demarcation mapping to design accelerated tests which will arguably reach end of life. A conservative value of $\nu$ for the purpose both of including processes running totally to completion, and some more complex processes is a value 3-orders of magnitude lower than what one would estimate is the lowest value for a simple single step chemical process in the materials under consideration. The minimum value of $\nu$ as described above is the index of coverage of the accelerated test for life stress. For every value of $\nu$ above that value, all reaction occurring during life will be reached.

## 4 Plausible physical effects in a model of the degradation process associated with fibre pistoning

### 4.1 General

The objective in this subclause is to list a series of plausible physical effects of degradation associated with fibre pistoning that can be used for demarcation approximation, and to illustrate the demarcation calculations for the simplest of these. The calculations will be done for an assumed service life of 20 years of a diurnal cycle between 20 °C, 70 % RH and 50 °C, 90 % RH, and compared with an accelerated cycle going between 25 °C, 85 % RH and 85 °C, 85 % RH. The diurnal cycle is approximated as four steps, 6 h each at the conditions: 20 °C and 70 % RH, 35 °C and 80 % RH, 50 °C, 90 % RH, and 35 °C, 80 % RH. The accelerated cycle has a 1 h dwell at 25 °C, 85 % RH and a 3 h dwell at 85 °C, 85 % RH, with a 2 h ramp between. The accelerated cycle is approximated as six steps with 1 h at 25 °C, 85 % RH, 1 h at 45 °C, 85 % RH, 1 h at 65 °C, 85 % RH, 3 h at 85 °C, 85 %, 1 h at 65 °C, 85 % RH, and 1 h at 45 °C, 85 % RH.

The possible physical effects associated with the above exposures include:

a) thermal degradation process;
b) direct action of moisture in terms of relative humidity, absolute humidity, or the effect of water accumulation at an interface;
c) diffusion of water into the actively degrading regions;
d) thermally induced mechanical stresses at interfaces;
e) thermally induced mechanical stresses within polymer adhesive;
f) the effect of cyclic fatigue on interfaces, and within the polymer.

In No.1 of Table 2, effects a) and b) were combined and in No.2 of Table 2, a) and b) (looking at absolute humidity only) were combined with c). In 3.1, delamination at the edge of the epoxy Equation (4) driven in part by thermal expansion mismatch is examined. Diffusion (Equation (3)) is not considered important, but temperature and humidity are considered as a function of a plausible model of an isotherm at an interface[12]. In No.4 of Table 2, the model used in No.3 of Table 2 is adapted to stress relaxation of the epoxy, assuming diffusion, temperature, and humidity as absolute humidity are important. In No.5 of Table 2, two approaches are considered to bound the effect of cyclic fatigue. One slightly more primitive, where some elements of the model of 4.4 are combined with a conservative approximate calculation of an acceleration factor based on a Coffin-Manson [15] model for hysteresis, and the other where a connection between the Coffin-Manson [15] model, and diffusion of defects in the polymer is proposed.

## 4.2 Simple temperature humidity models

In this simplest case the effects of diffusion and of differential mechanical stress acting at different temperatures are ignored. The rate of reaction is assumed to have the form:

$$k_1 = \nu f(RH,T)\exp\left(\frac{-E_a}{\mathbf{k}T}\right) \tag{8}$$

where

$$f(RH,T) = \begin{cases} (RH)^\beta \\ (\text{vapour pressure})^\beta \\ \left(\dfrac{RH}{1-RH}\right)^\beta \end{cases} \tag{9}$$

depending on the physics. The Equation (9) was derived to model the number of monolayers of gas adsorbed on a surface [6]. This expression is useful in dealing with reactions rates occurring at material interfaces. The other two are used often, although careful derivations of which situations are most appropriate for which model are not available. The assumption is made that β is 1 for now.

Equation (8) results in a definition of demarcation energy with the form:

$$E_a = \mathbf{k}T \ln(\nu f(RH,T)\,t) \tag{10}$$

From this, a similar result to that given in Equations (5), (6), and (7) can be derived so that after a step in stress, the demarcation energy may be calculated:

$$E_a = \mathbf{k}T_2 \ln\left(\nu\left(t_2 + \frac{\left(\nu f(RH_1,T_1)t_1\right)^{T_1/T_2}}{\nu f(RH_2,T_2)}\right)\right) \tag{11}$$

Using Equations (9), (10), and (11), demarcation maps were constructed comparing 20 years of the diurnal cycle with 200, 600, and 2 000 cycles respectively of the accelerated cycle. Table 1 below gives the results of that comparison in terms of index of coverage. The index of coverage is given as the common log of $\nu$ (in Hz) where service life and accelerated test maps intersect. Below this value, reactions in service will not be activated by the accelerated test, assuming the validity of the assumptions in the model.

**Table 1 – Accelerated test index of coverage for simple temperature-humidity model**

|  | Number of cycles in accelerated test | | |
|---|---|---|---|
|  | 200 | 600 | 2 000 |
| Relative humidity | 11 | 8 | 2 |
| Vapour pressure | 6 | 2 | -3 |
| Surface adsorption | 12 | 7 | 2 |

Since values of $\nu$ on the order of $10^8$ Hz are quite common, the defined accelerated test does not give good coverage of potential service life reactions for less than about 2 000 cycles in the accelerated regime. However since the model this models assumes no

differential effect of thermally induced mechanical stresses, or of diffusion in the degradation process, it may be oversimplified.

Further, it should be noted that a more efficient similar aging effect for this failure mode is provided by simply soaking the devices at 95 °C, 85 % RH for 2 000 h.

## 4.3    Temperature humidity models with diffusion

In this subclause, the effects of differential mechanical stress acting at different temperatures are ignored, but diffusion is included. The rate of reaction is assumed to have the form:

$$k_1 = vD\big(f(RH,T),T,t\big)\exp\left(\frac{-E_a}{kT}\right) \tag{12}$$

where

$f(RH,T)$ is the vapour pressure, and

$D(f,T,t)$ is the diffusion process.

It is assumed that the primary effect of the water is in the epoxy, and the diffusion proceeds from the ends of the cylinder of epoxy inward. This is equivalent to linear diffusion along a line. To make this most convenient with other kinetic modeling, diffusion is treated as reversible transport through a series of compartments. A refinement to this approach would be to look at the effect of exact kinetic-diffusion solutions.

By adding diffusion, the character of the system is changed in two ways. The diffusion is assumed to drive towards an equivalent equilibrium between the vapour pressure of water in the air, and concentration of water in the epoxy (which is why the model is confined to vapour pressure). This results in a few things. The concentration of water changes with the cycling, and the concentration of water in the epoxy at the lower temperatures of the cycle can be much higher than the concentration of water attainable by soaking the epoxy at the same low temperature in the same relative humidity.

Assuming that the reaction rate is proportional to the concentration of water in the system and make the following bounding arguments simplifies the calculation. Diffusion will lead to a quasi steady state where each part of the cycle will have a characteristic water concentration, after the initial transient as water moves into the system. What this steady state looks like, and how long it takes to get there depends of course on assumed diffusivity and activation energy of diffusion. To provide a conservative bound on coverage, while still allowing fast calculation of bounds, this steady state gives an over estimate of the demarcation energy reached by the life stress exposure, and an under estimate of the experimental stress exposure. This is done by assuming that under life stress, the eventual steady state is reached immediately, while under accelerated stress, the total number of cycles is decreased to match the actual time when steady state is reached.

Four different combinations of "pseudo-diffusivity", and activation energy in the compartment model are considered (The pseudo diffusivity was just the premultiplier for the Arrhenius rate to move between compartments). The pairs, listed as (diffusivity (Hertz), activation energy (eV)) are (1e12;1), (1e11;0,9), (1e6,5;0,6), and (1e5;0,6). No. 2 in Table 2 shows that again, to be conservative it is necessary to approach 2 000 cycles.

## 4.4    A model of delamination

In this case, the effects of differential mechanical stress acting at different temperatures are included as a simplified model of creep using the approach of Krausz and Erying [13]. Instead of the process being a simple first order reaction, the assumption is made that at each local site of reaction, it is reversible and that the process is only reversible for a short time along the delamination front. Infinitesimally, the process looks like:
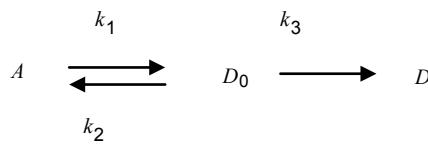
**Figure 3 – Schematic for the delamination process**

The rate of reaction in each direction between $A$ and $D_0$ is assumed to have the form:

$$k_i = vf(RH,T)\exp\left(\frac{-(E_a \mp a(T - T_0))}{kT}\right)$$ (13)

where

$A$   denotes the undamaged configuration,

$D_0$ denotes the reversibly damaged configuration, and

$D$   denotes the irreversibly damaged configuration.

The + associated with the activation energy is for the healing direction of the process (backward), and the minus is for the damaging direction (forward). $f(RH,T)$ is the interface function from 4.2. $a$ is a scaling factor that changes the temperature difference to an effect on the activation energy of the forward and backward process. For simplicity, it is assumed that at any given site the forward and backward activation energies are identical, as are the values of $v$.

For the purpose of building a physical model, it is assumed that the step represented by $k_3$ is significantly slower than that represented by $k_1$ and $k_2$ during constant temperature and humidity, but is significantly faster when the temperature and/or humidity changes. So on a short time scale, delamination is reversible at the delamination front, but over changing temperature and humidity the conformation of the two surfaces changes enough so the delamination becomes essentially irreversible. Still assuming that the stepwise approximation of the cycling is reasonable, if the degradation equations are solved as reversible equations with $k_3$ set equal to 0 during stress, then the step transition resets $D_0$ to 0. Thus during the "constant temperature regimes" the accumulation of degradation is modelled as:

$$D = \left[\left(\frac{k_1}{k_1 + k_2}\right)(1 - \exp(-(k_1 + k_2)t))\right]A_0$$ (14)

Applying Equation (13) and the definition:

$$z = \frac{a(T - T_0)}{kT}$$

then Equation (14) can be rewritten as:

$$D = \left[\left(\frac{1}{1 + \exp(-2z)}\right)\left(1 - \exp\left(-\left([v(\exp(z) + \exp(-z))]\exp\left(-\frac{E_a}{kT}\right)\right)t\right)\right)\right]A_0$$ (15)

Recall from 4.1 that the approximation is defined when

$$\frac{D}{A_0} = 1 - \exp(-1)$$

Equation (15) however has two components, and asymptote that does not vary under constant stress $\left( \dfrac{1}{1 + \exp(-2z)} \right)$ and the time varying portion

$$\left( 1 - \exp\left( -\left( [\nu(\exp(z) + \exp(-z))] \exp\left( -\frac{E_a}{kT} \right) \right) t \right) \right)$$

If the asymptote is less than 1-exp(-1), then the demarcation energy is never reached using this definition. However, thinking physically, the notion of the demarcation energy allowing us to separate time scales is still valid, even if the total degradation is limited. There are several plausible ways to define the demarcation approximation in this case. One is the following:

$$\Delta(k,t) = \begin{cases} 1 \text{ if condition A or B holds} \\ 0 \text{ otherwise} \end{cases}$$

where

condition A is : $\left\{ \dfrac{D}{A_0} > 1 - \exp(-1) \right\}$ and $\left\{ \left( \dfrac{1}{1 + \exp(-2z)} \right) > \dfrac{1 - \exp(-1)}{1,01} \right\}$

condition B is : $\left\{ \dfrac{D}{A_0} > \dfrac{1 - \exp(-1)}{(1,01)(1 + \exp(-2z))} \right\}$ and $\left\{ \left( \dfrac{1}{1 + \exp(-2z)} \right) \leq \dfrac{1 - \exp(-1)}{1,01} \right\}$

To define the transformation between conditions, the demarcation energy is not allowed to decrease. This is equivalent to assuming that there is no real way for the system to heal, and that it is always degrading (if slowly) under any condition. Then the transformation between conditions is defined by the above criterion, plus the necessity that the demarcation energy never decrease. The demarcation energy numerically based on these definitions as follows.

In the numerical experiments with this model, two new parameters, $a$ and $T_0$ that can be varied during simulation. In this case, $T_0$ is assumed to be 20 °C, so that at all conditions above 20 °C, mechanical stress is increasing the reaction rate. The effect of setting $a$ to 0,002 (in which case 60° temperature swing is equivalent to reducing the activation energy by 0,12 eV) and 0,01 (in which case the same 60° reduces the activation energy by 0,6 eV) are investigated. In addition, linear vs. quadratic effects of the concentration of water at the interface are considered to see if that changes how the index of coverage changes. No. 3 in Table 2 shows the results.

It should be noted that in this model, for the parameters investigated, the acceleration is far more effective than in the previous two models that ignore the effect of mechanical stress on the degradation process. In this case 200 cycles is sufficient.

## 4.5 A model of stress relaxation

In this subclause, the exercise used in the previous subclause is repeated except that degradation occurring in the bulk epoxy is considered rather than at the interface of the epoxy and the ferrule or the glass. A similar model to that above is used with the added constraint that the degradation is constrained by presence of "conformers" in the bulk epoxy [14]. The

Matsuoka and Quan model [14] of conformer interaction implies that within a polymer, around and below $T_g$, the ability of polymer strands to slip past one another is constrained by the polymers strands around them. The size of the neighborhood is influenced by the temperature, and at $\widetilde{T}$ which is 50 °C below $T_g$, the size of the neighborhood becomes infinite, so creep does not happen. The model they use to describe this behaviour is to transform the activation energy of the creep process, multiplying the activation barrier by the number of molecules coupled together in any movement. The units of coupled molecules are called conformers.

The formula for the average number of molecules in a conformer neighborhood assuming a dry material is:

$$z(T) = \frac{T^*\left(T - \widetilde{T}\right)}{T\left(T^* - \widetilde{T}\right)} \tag{16}$$

where

$T^*$     is around 500 °C, and

$\widetilde{T}$     is 50 °C below $T_g$.

If it is assumed that $T_g$ is linearly dependent on partial vapour pressure which in turn is proportional to absolute humidity, then Equation (16) can be modified to:

$$z(T, RH) = \frac{T^*\left(T - \left(\widetilde{T} - \alpha \times [H_2O]\right)\right)}{T\left(T^* - \left(\widetilde{T} - \alpha \times [H_2O]\right)\right)} \tag{17}$$

with $[H_2O]$ simply the concentration of water in the polymer, which is assumed proportional to the vapour pressure.

With this adjustment Equation (13) can be modified to:

$$k_i = vf(RH, T)\exp\left(\frac{-\left(\left(E_a z(T, RH)\right) \mp a\left(T - T_0\right)\right)}{kT}\right) \tag{18}$$

A few moments inspection reveal that Equation (18), and the subsequent derivations paralleling Equation (15) and what follows in No.3 of Table 2, will in fact make the relative acceleration as a function of temperature even faster than that given by the delamination process proposed in the previous subclause. Numerical calculations were made with an $a$ value of 0,002, $T_g$ values of 80 °C and 120 °C, and $\alpha$ values of 0,1 and 30. The latter correspond to drops in $T_g$ of between 0,057 to 18° at 85 °C, 85 % RH. With these values the index of coverage was less than –5 for even 20 cycles of the accelerated condition.

## 4.6   Two models bounding cyclic hysteresis

In this subclause, the assumption is made that the main effect of hysteresis is in the polymer, and that like hysteresis in metals [15], the effect on time is superlinear with plastic strain. A paper by N. E. Iwamoto [16] notes that a Coffin-Manson like relationship does exist in polymers at the molecular level.

If the effect on time is superlinear with plastic strain (e.g. time goes up faster than the inverse ratio of plastic strains) than a conservative acceleration factor between two conditions is the ratio of plastic strains. Assuming that the plastic strain is proportional to the stress relaxation times the time for relaxation and that the stress relaxation may be modelled molecularly using Equations (14) and (18), the ratio of plastic strains at each condition is:

$$acceleration.ratio = \frac{k_1(\text{low stress}) \times t_{\text{relaxation low stress}}}{k_1(\text{high stress}) \times t_{\text{relaxation high stress}}} \tag{19}$$

The assumption is made that only $k_1$ is important because only relatively short times are considered. To be conservative, the rate constant is taken to be that at highest stress of the cycle, the relaxation time at high stress to be 3 h, and the relaxation time at low stress to be 24 h. The number of cycles at high stress which is equivalent under this formulation, to the number of cycles at low stress is simply the number of cycles at low stress times the acceleration ratio. In this formulation, which is unfortunately oversimplified, the effect of $v$ cancels out.

Eliminating any case where the plastic strain drops to 0 at the life condition (because in this case, accelerated aging will only induce artificial failure modes), the number of cycles at end of life are calculated over the region for activation energies between 0,1 and 2 eV, for values of $a$ between 2e-5 and 2e-3, for values of $Tg$ between 80 °C and 120 °C. For values of $T_0$ between 10 °C and 30 °C and for values of $\alpha$ between 0,1 and 30, the maximum number of cycles at the high stress to reach an end of life condition was less than 240. *(Note by relying on acceleration factors, some of the bounding theory available for demarcation maps is lost* [1]*)*.

An alternative analysis is possible proposing a theoretical model of the effect giving rise to the empirical Coffin-Manson relationship. Such a model needs to be checked by careful experimentation. The classical Coffin-Manson relationship has the form:

$$\varepsilon_p = M N_f^z \tag{20}$$

where

$\varepsilon_p$     is the asymptotic plastic strain per cycle,

M     is a material dependent constant,

$N_f$     is the number of cycles to failure, and

$z$     is typically –1/2 for materials like steel.

In the most simplistic view, plastic strain should be proportional to the movement of any defects from way they are generated, through the material. If the total movement by the end of each cycle is random, then the total concentration at the end of $N$ cycles at any particular position from the point of origin is proportional to $N^{1/2}$, assuming independent movements.

Using the same approximation as above for plastic strain, that is the stress relaxation rate constant times time, Equation (20) can be arranged to have the form

$$\left( \frac{D_0 \times time_{relaxation}^2 \times k_1^2}{M^2} \right) N_f = 1 \tag{21}$$

This is exactly the same form as used in Equation (3), with $\left( \dfrac{D_0 \times time_{relaxation}^2 \times k_1^2}{M^2} \right)$ in place of $k_1$ and $N_f$ in place of $t$. A demarcation map is directly derived from Equations (18) and (21) for the number of cycles.

If $v*\left(time^2\right)$ denotes the product $\left( \dfrac{D_0 \times time_{relaxation}^2 \times v^2}{M^2} \right)$ then the equation corresponding to (4) is: